Meteorol Atmos Phys (2012) 115:1–13
DOI 10.1007/s00703-011-0170-8

ORIGINAL PAPER

On the role of cloud adjustment time scale in simulating precipitation with Relaxed Arakawa–Schubert convection scheme

Deepesh Kumar Jain · Arindam Chakraborty · Ravi S. Nanjundiah

Received: 11 April 2011 / Accepted: 11 November 2011 / Published online: 23 November 2011
© Springer-Verlag 2011

Abstract The precipitation by Relaxed Arakawa–Schubert cumulus parameterization in a General Circulation Model (GCM) is sensitive to the choice of relaxation parameter or specified cloud adjustment time scale. In the present study, we examine sensitivity of simulated precipitation to the choice of cloud adjustment time scale (τ_{adj}) over different parts of the tropics using National Center for Environmental Prediction (NCEP) Seasonal Forecast Model (SFM) during June–September. The results show that a single specified value of τ_{adj} performs best only over a particular region and different values are preferred over different parts of the world. To find a relation between τ_{adj} and cloud depth (convective activity) we choose six regions over the tropics. Based on the observed relation between outgoing long-wave radiation and τ_{adj}, we propose a linear cloud-type dependent relaxation parameter to be used in the model. The simulations over most parts of the tropics show improved results due to this newly formulated cloud-type dependent relaxation parameter.

Keywords RAS convection scheme · General Circulation Model · Cloud adjustment time scale · Monsoon precipitation

1 Introduction

Parameterization of interaction between various components of the climate system has significant impact on the uncertainty of weather and climate prediction from daily to decadal time scales (Tebaldi and Knutti 2007). One of the most important variables in weather prediction, the precipitation, results from various types of clouds and moist convection process. The east Asian and Indian monsoon areas are the regions of most active convection on earth (Ratnam et al. 2009; Das et al. 2001), and intensity variations of convection at intraseasonal time scales can produce droughts and floods over these regions (Bhanu Kumar et al. 2010). The simulation of precipitation in these regions by any numerical weather prediction (NWP) model depends on the cumulus parameterization scheme and various parameters that govern different processes in these schemes (Pattanaik 2004; Tiedtke et al. 1988; Zhang and McFarlane 1995; Sperber and Palmer 1996; Martin and Soman 2000; Rajendran et al. 2002; Ratnam and Kumar 2005).

One of the most significant work in the field of cumulus parameterization was done by Arakawa and Schubert (1974) (in developing the Arakawa–Schubert convection scheme; AS hereafter), and Anthes (1977) and Krishnamurti et al. (1980) (development and modification of the Kuo convection scheme). However, the implementations of original ideas of AS (Lord and Arakawa 1980) was computationally expensive. Simple implementation of AS parameterization, such as Relaxed Arakawa Schubert (RAS) by Moorthi and Suarez (1992) (hereafter MS) and Simple Arakawa–Schubert (SAS) developed by Grell (1993) and Pan and Wu (1995), were subsequently proposed. There are many parameters in RAS such as re-evaporation ratio, critical cloud work function and convective adjustment time scale (τ_{adj}) that govern the precipitation process. Pattanaik (2004) studied the impact of specifying different values for critical cloud work function and re-evaporation ratio in RAS using Center for Ocean–Land–Atmosphere (COLA) studies GCM. The excessive rainfall over the Bay of Bengal (BoB) decreased by

Responsible editor: S. Hong.

D. K. Jain · A. Chakraborty (✉) · R. S. Nanjundiah
Centre for Atmospheric and Oceanic Sciences and Divecha Centre for Climate Change, Indian Institute of Science, Bangalore, India
e-mail: arch@caos.iisc.ernet.in

modifying the values of cloud work function and revaporation ratio.

Studies by Mishra and Srinivasan (2010) and Lee et al. (2009) suggest that the choice of τ_{adj} has major impact on the simulations of precipitation. Mishra and Srinivasan (2010) examined the sensitivity of simulated precipitation to the choice of convective relaxation time in Zhang and McFarlane (1995) cumulus parameterization using Community Atmospheric Model version 3 in an aqua-planet configuration. They found that increasing the value of τ_{adj} decreased the deep convective precipitation which led to the accumulation of moisture content in the atmosphere. This led to the increase in shallow convective and large-scale precipitation which acted to cap the accumulated convective instability. They showed that setting τ_{adj} to 8 h, instead of conventionally used value of 1–2 h, produced better simulations.

In RAS, the effect of τ_{adj} is taken into account using a relaxation parameter. MS presented results for the evolution of cloud work-function, total precipitation, entrainment parameter and precipitation rate for different fixed values of relaxation parameters in their 9-layer model. They found that the process of adjustment to equilibrium state is sensitive to the choice of relaxation parameter. Increased number of iterations (and hence more clouds) were needed to adjust the environment to equilibrium state when a smaller relaxation parameter was selected. Furthermore, a smaller relaxation parameter gave lower precipitation rates. MS also showed that the rate of change of entrainment parameter could be neglected in kernel calculation if a smaller relaxation parameter was selected. MS compared the evolution of precipitation rate, vertical heating and drying profiles by RAS with GARP (Global Atmospheric Research Program) Atlantic Tropical Experiment (GATE) phase III data using semi-prognostic and prognostic tests. Although MS emphasized a cloud-type-dependent relaxation parameter, they used only one fixed value of relaxation parameter for all cloud types.

In the present study, we examine the effect of relaxation parameter on the spatial distribution of simulated precipitation by a GCM. The next section describes the model used for the experiment. In Sect. 3, we discuss the role of relaxation parameter in RAS in controlling the grid scale precipitation. Section 4 provides the experimental details. The observational data sets used for validating the results are discussed in Sect. 5. Section 6 discusses our results of this study followed by summary of our conclusions.

2 Model description

The NCEP's Seasonal Forecast Model (SFM) is used for the present study at T62L28 resolution. The corresponding horizontal resolution near the Equator is about 1.875° in both longitude and latitude directions. It has 28 unequally spaced vertical sigma levels. The model uses reduced grid near the poles for uniform resolution throughout. The short-wave radiation parameterization is based on Chou (1992). The long-wave parameterization is based on Chou and Suarez (1994). Cloud fraction is determined using the scheme of Slingo (1987). Planetary boundary layer parameterization is by Hong and Pan (1996). Mountain-induced gravity wave drag parameterization by Alpert et al. 1988 and land process parameterization by Pan and Mahrt (1987) is used in the model. The orography is smoothed mean and ozone is given using climatology. The cumulus scheme is based on Moorthi and Suarez (1992). Model dynamics is based on semi-implicit time integration scheme. More details about the model can be found in Kanamitsu et al. (2002).

3 Relaxed Arakawa–Schubert parameterization

The RAS used in the present study is based on the theory of Moorthi and Suarez (1992). In this scheme, a cloud type is distinguished by the height at which it detrains. It is assumed that all the liquid water is carried to the cloud top and then a fraction is precipitated and remainder is evaporated in the environment.

3.1 Role of relaxation parameter in controlling precipitation rate

In this section, we briefly discuss the role of relaxation parameter in controlling precipitation rate in RAS. The major simplifications made by MS include that rather than the final state be balanced (quasi-equilibrium in AS sense), the environment is relaxed towards quasi-equilibrium every time the parameterization is called. Multiple cloud types are called for a single time step, one after the other and each cloud type relaxes the environmental state towards quasi-equilibrium. The amount of relaxation depends on the iteration time step, the prescribed time scale (MS) and the frequency with which each cloud type is called. If Δt is the iteration time step and τ_{adj} is the cloud adjustment time scale (10^3–10^4 s according to AS), then the relaxation parameter is given by (Moorthi and Suarez 1992)

$$\alpha = \triangle t/\tau_{adj}. \quad (1)$$

The cloud adjustment time scale is cloud type dependent and hence the relaxation parameter (α) is cloud-type-dependent.

In RAS, the environmental potential temperature θ and specific humidity q are the prognostic variables. According to MS, a cloud type is identified by the level at which it

detrains. In a K-layer model, suppose a cloud type detrains at the ith level, then it is the ith cloud type. The rate of change in the potential temperature (θ) and specific humidity (q), due to ith cloud sub-ensemble is calculated as

$$\left(\frac{\partial\theta}{\partial t}\right)_{\mathrm{c}} = \alpha\frac{m_{\mathrm{B}}(\lambda_i)\triangle\lambda_i}{c_{\mathrm{p}}P}\Gamma_{\mathrm{s}}(P), \tag{2}$$

and

$$\left(\frac{\partial q}{\partial t}\right)_{\mathrm{c}} = \alpha\frac{1}{L}m_{\mathrm{B}}(\lambda_i)\triangle\lambda_i[\Gamma_{\mathrm{h}}(P) - \Gamma_{\mathrm{s}}(P)], \tag{3}$$

and the liquid–water mixing ratio at the top of the detrainment level is given by

$$\begin{aligned} l(P_{\mathrm{D}}) &= l^{\mathrm{c}}_{\lambda}(P_{\mathrm{D}}) \\ &= \frac{1}{\eta_{\lambda}(P_{\mathrm{D}})}\left[q(P_{\mathrm{B}}) + \frac{c_{\mathrm{p}}}{g}\lambda\int_{P_{\mathrm{D}}}^{P_{\mathrm{B}}}\theta q(P)dP\right] - q^{*}(P_{\mathrm{D}}) \end{aligned} \tag{4}$$

where, $l(P_{\mathrm{D}})$ is the liquid–water mixing ratio of the cloud air detraining at pressure level P_{D} of the ith cloud type, $\eta_{\lambda}(P_{\mathrm{D}})$ is the normalized mass flux in the cloud at P_{D} normalized by the value at the cloud base, $q(P_{\mathrm{B}})$ is specific humidity at the cloud base, λ is the fractional entrainment rate, $q^{*}(P_{\mathrm{D}})$ is the saturation specific humidity at P_{D}. $\Gamma_h(P)$ and $\Gamma_s(P)$ are the tendencies of the environmental moist static energy h and dry static energy s per unit cloud base mass flux given by Equations 27 and 28 in Moorthi and Suarez (1992).

The precipitation is parameterized as

$$R_i = m_{\mathrm{B}}(i)r_i l_i \tag{5}$$

where, R_i is precipitation, m_B is the cloud base mass flux, l_i is liquid–water mixing ratio due to ith cloud type, and r_i is cloud-type-dependent parameter given by

$$r_i = 1.0, \quad \text{if } p_i < 500 \tag{6}$$

$$r_i = 0.80 + \frac{800 - p_i}{1500}, \quad \text{if } 500 < p_i < 800 \tag{7}$$

$$r_i = 0.80 \quad \text{if } p_i > 800 \tag{8}$$

where, p is pressure in hPa.

As it is seen from Eqs. (2), (3) and (4), the choice of relaxation parameter affects the rate of change of q and θ and hence liquid–water mixing ratio $l(P_{\mathrm{D}})$ during each iteration. The term inside the integral in Eq. (4) makes the relation between $l(P_{\mathrm{D}})$ and α a nonlinear one. Hence, it can be inferred from Eq. (5) that R_i varies as α is varied in a nonlinear fashion.

4 Experimental details

We have used a time step of 30 min for our experiments. In the default configuration of the model α is 0.30, corresponding to cloud relaxation time of the order of 100 min. We call this case ($\alpha = 0.30$) the control experiment. Further simulations were performed for different values of α and a cloud-type-dependent α. Brankovic and Palmer (1997) suggested that an ensemble size of 5–10 assures high-potential predictability for seasonal precipitation over the Indian region and hence ensemble simulations were performed with the model. The model integrations were performed for 5 initial conditions starting from 27 to 31 March, each day corresponding to 1 initial condition. The model was integrated till 30 September. The results shown in the following sections are mean of five ensembles. SST (monthly mean) are specified from Reynolds and Smith (1994) and the values are interpolated linearly to model the time step. Initial conditions are taken from NCEP. The focus of the present study is to test the sensitivity of simulated precipitation over the tropics during Indian summer monsoon (ISM) season (June–September). We choose a year with near normal rainfall over Indian land during the same period. According to Indian Meteorological Department, rainfall over Indian land was near normal (98% of climatological mean) for the period from June to September, 2008 and hence year 2008 is selected for the experiment. For the experiment, the model output is saved as a daily average.

5 Data sets

Precipitation over Indian land and southeast Asia is maximum during June–September of every year. To compare precipitation over Indian land, rain gauge data provided by Indian Meteorological Department (IMD) is sufficient. However, IMD's data is available only over the Indian landmass and therefore to validate results over the tropics, global data sets such as TRMM 3B42 and GPCP (gauge and satellite merged) are used here. 3B42 is a level three data available at a horizontal resolution of 0.25° × 0.25°, has a temporal resolution of 3 h available from 1998 onwards and a geographic coverage between 50° S–50° N. 3B42 rainfall product (e.g., see Kummerow et al. 1998; Adler and Huffman 2000; Huffman and Adler 2007) is an optimal combination of various high-quality microwave estimates to adjust infrared estimates from high-frequency geostationary observations. For making comparisons, the data are regridded to the model's T62 resolution, and is averaged over a day. GPCP's satellite-gauge combined data is available at a horizontal resolution of 2.5° × 2.5°. GPCP version 2.1 combined precipitation data is available as long-term monthly mean and has temporal coverage from January 1979 to September 2009. It has a resolution coarser than that of the model grid and covers the entire globe. Figure 1 shows the spatial correlation (SC) between

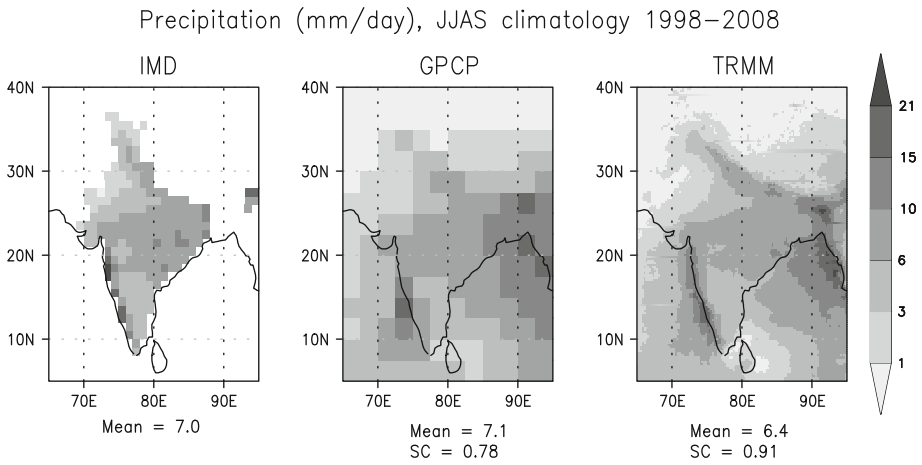

Fig. 1 Climatology mean of precipitation from three data sets over Indian region for the period of June– September, 1998–2008. For calculation of the spatial correlation (SC) and mean precipitation, data from TRMM and GPCP are regridded to IMD resolution and is considered only over the points where IMD shows positive precipitation

TRMM and IMD climatology (Fig. 1: right panel) and between GPCP and IMD climatology (Fig. 1: middle panel) for the period of June–September, 1998–2008. The SC between the two patterns of rainfall is calculated as

$$\mathrm{SC} = \frac{\sum_{i,j}(x_{i,j} - \overline{x})(y_{i,j} - \overline{y})}{\sqrt{\sum_{i,j}(x_{i,j} - \overline{x})^2 (y_{i,j} - \overline{y})^2}} \tag{9}$$

where, x and y refer to the variable in the first and the second data set, i and j represent the grid point index of the region under consideration, $\overline{x}$ and $\overline{y}$ are the spatial averages of first and the second data set respectively. For calculations, we only consider those points where IMD's data is available (Fig. 1). It is clear that TRMM (SC = 0.91) is closer to IMD when compared to GPCP (SC = 0.78). Based on this analysis, we choose TRMM estimated precipitation as the observed data set to compare model outputs in this paper.

6 Results

6.1 Mean spatial patterns of precipitation in control simulation

The comparison between the spatial patterns of climatology of JJAS mean precipitation over the tropics during the period 1998–2008 in model and observation respectively, is presented in Fig. 2. The model simulates a distinct intertropical convergence zone (ITCZ) north of the equator over eastern Pacific and dry subtropical regions over the Sahara deserts. The mean SC between simulated tropical rainfall (30° N–30° S,0° E–360° E) and observations (GPCP and TRMM) is greater than 0.7, which is appreciable considering the fact that the SC between the two observational data sets (GPCP and TRMM) is 0.85. The root mean square error (RMSE) mentioned in Fig. 2 is calculated with respect to TRMM as

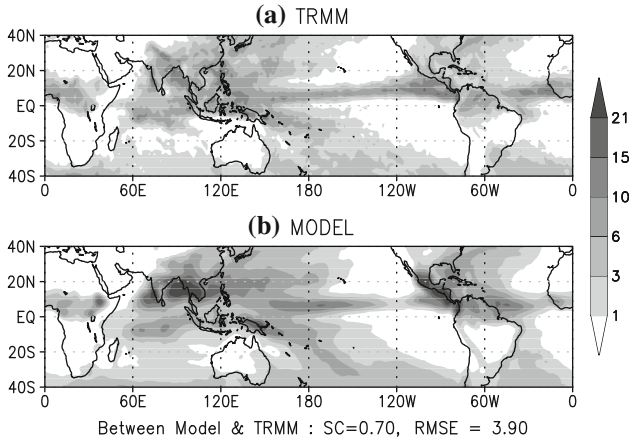

Fig. 2 Precipitation climatology (mm day^{-1}) during June–September of 1998–2008 from TRMM estimates and model control simulation. The spatial correlation (SC) and root mean square error (RMSE) are calculated for the region 30°S–30°N, 0°E–360°E

$$\mathrm{RMSE} = \sqrt{\sum_{i,j} \frac{(X_{i,j} - O_{i,j})^2}{N}} \tag{10}$$

where, O and X refer to the variable in observed data set and model respectively, i and j represents the grid point index of the region under consideration. N is the total number of grid points under consideration. RMSE is 3.24 mm day^{-1} between model and observation which is significantly high.

Figure 3 gives climatology mean values of precipitation over different parts of tropics during June–September. The precipitation is overestimated over the Western Pacific (WP), American tropics, Bay of Bengal (BoB), Indian landmass and central Africa. However, over the equatorial Indian Ocean (EIO), the model underestimates precipitation. The intercomparision of simulated precipitation between ten GCMs over the northern hemisphere summer by Kang et al. (2002) showed that several models with

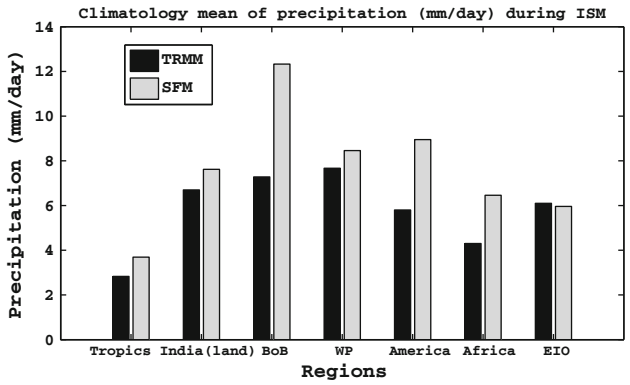

Fig. 3 Area mean climatology of the precipitation during June–September of 1998–2008 over different parts of the tropics from TRMM estimates and model control simulation

various convection schemes produced excessive rainfall over southeast Asian and Indian region. SFM also overestimates the precipitation over these regions.

6.2 Simulations with different values of relaxation parameter

It was seen in Sect. 3 that the choice of value of relaxation parameter (α) is critical in determining the precipitation rate in the RAS convection scheme. To understand its impact, we investigate the sensitivity of simulated rainfall with relaxation parameter values 0.10, 0.20, 0.40, and 0.50. Since the model time step is 30 min, these values correspond to cloud relaxation time of 300, 150, 75, and 60 min.

Figure 4 shows the comparison between mean spatial patterns of JJAS precipitation over the tropics with different relaxation parameter values. Irrespective of the value of the relaxation parameter, a narrow precipitation belt along the ITCZ is realistically simulated over the Pacific in all cases. SC is highest for $\alpha = 0.30$ and RMSE is least for $\alpha = 0.20$. The simulated precipitation over central Africa, WP, southeast Asia, India, BoB, EIO and Amazon is sensitive to the choice of the relaxation parameter. Over central African and Indian landmasses, the spatial coverage and magnitude of precipitation increases as α decreases. The magnitude of precipitation decreases over BoB, southeast Asia and WP as α decreases. Over the American tropics, the spatial pattern of precipitation is less affected by the choice of relaxation parameter. However, its magnitude increases (especially over Amazon) as α decreases.

It can be inferred from Fig. 4 that the choice of α has maximum impact on the magnitude of precipitation over India, southeast Asia, and WP. Since maximum precipitation occurs in India and southeast Asia during JJAS, we analyze the effect of α over these regions. Over the Indian landmass (8° N–28° N,70° E–90° E), the choice of α has

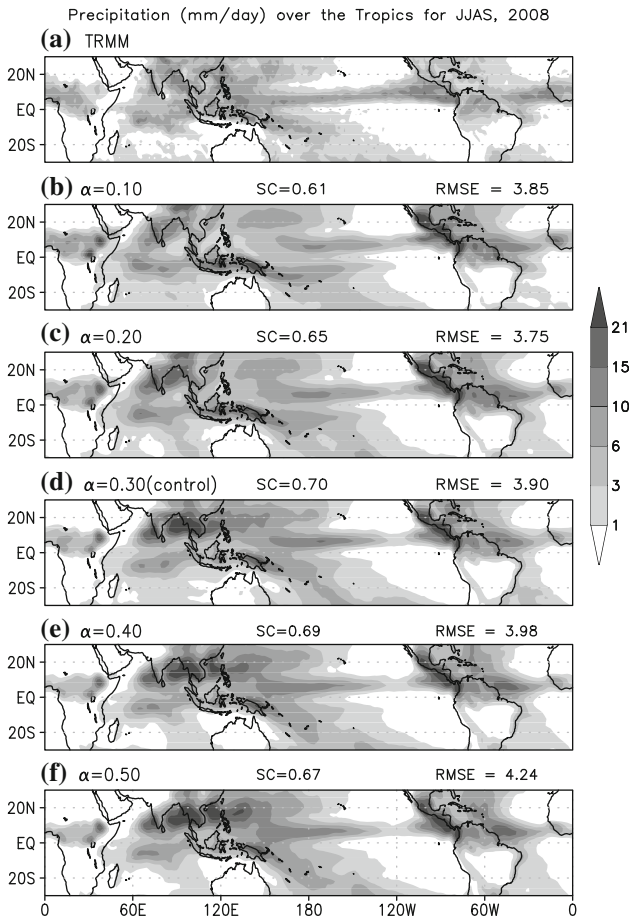

Fig. 4 Precipitation during June–September 2008 from TRMM estimates and model simulation with different relaxation parameters. The spatial correlation (SC) and root mean square error (RMSE) are indicated at the top of respective panels

significant effect on the variation of precipitation with time. Figure 5 shows the observed (TRMM) and model simulated time series of mean precipitation over the Indian landmass during JJAS, 2008. The observed TRMM precipitation shows active and break spells during JJAS. However, these spells could be absent in the model results due to ensemble averaging. Chakraborty et al. (2002) defined the onset of Indian summer monsoon as the day when the mean precipitation over the Indian landmass exceeds threshold of 3.5 mm day^{-1} and persist above the threshold for at least one pentad. In the present study, we use the same criteria to define the onset of monsoon over the Indian landmass. According to TRMM, the onset occurs on 1 June. For $\alpha = 0.10$, the onset occurs one day in advance (31 May). For $\alpha = 0.20$, the onset is delayed by 2 days (3 June). The control value of relaxation parameter, $\alpha = 0.30$, gives onset on 31 May even though the precipitation does not really escalate to the higher values observed in TRMM till as late as 16 June. For values of α of 0.40 and 0.50, the onset occurs on 7 and 21 June,

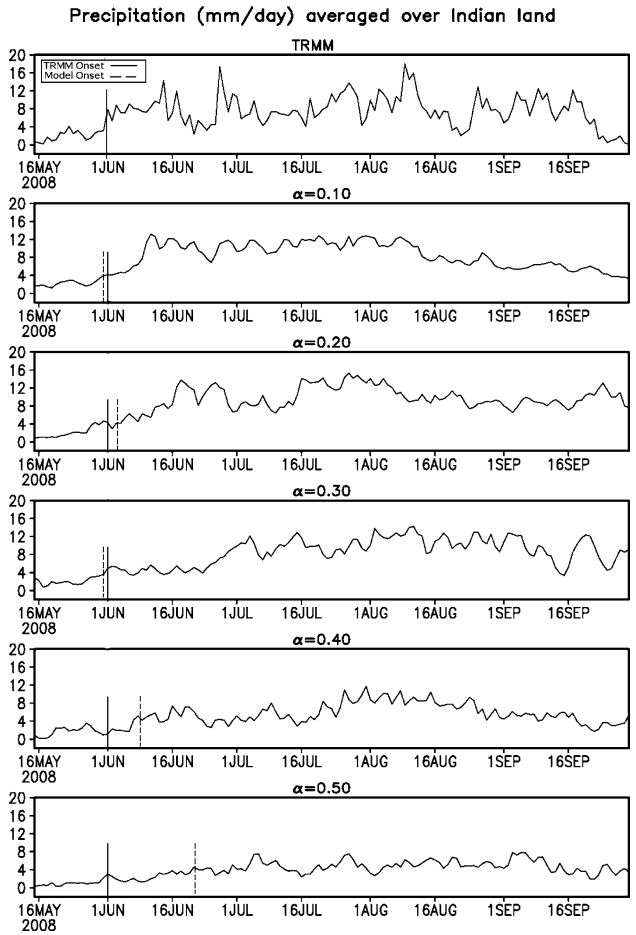

Fig. 5 Time series of precipitation over Indian land mass (70°–90°E, 8°–28°N) from TRMM estimates and model simulations with different relaxation parameters. Also indicated, by *vertical lines*, are the onset dates of all-India monsoon (criteria defined in text)

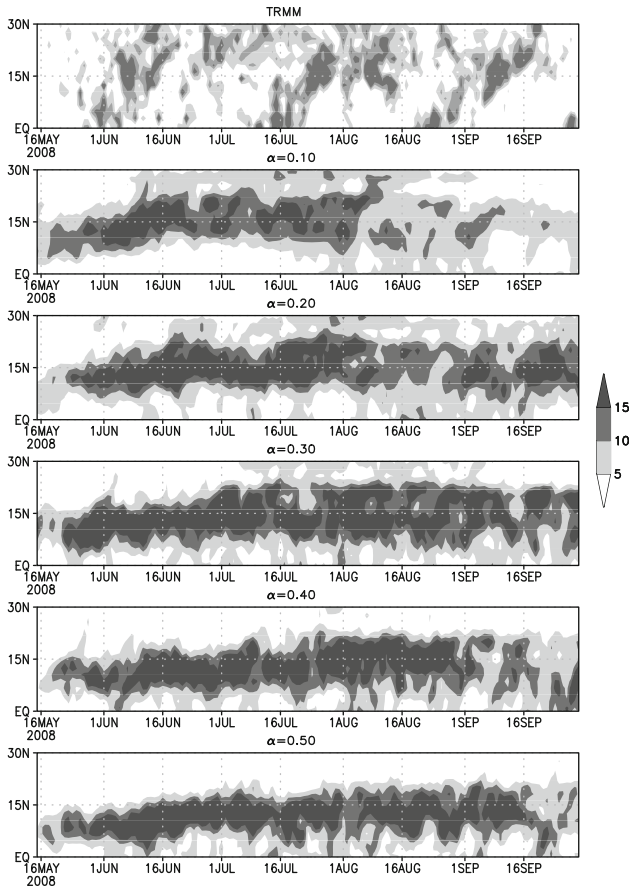

Fig. 6 Observed and model simulated latitude-time plot of precipitation (mm day^{-1}) averaged between 80°–90°E

respectively. This shows that the onset date is very sensitive to values of α higher than 0.30 and not very sensitive to values of α less than 0.30. Furthermore, for $\alpha = 0.50$, the mean precipitation never exceeds 8 mm day^{-1} during the season and oscillates around the threshold (3.5 mm day^{-1}) which is far from observation (TRMM).

Ensemble mean latitude versus time plot of precipitation averaged over 80° E–90° E during JJAS 2008 is shown in Fig. 6. In observations, we see the active and break spells of precipitation bands. Only for $\alpha = 0.10$, these bands are simulated in the model over the region and precipitation decreases after 10 August as seen in observations. The northward extent of precipitation is also sensitive to the choice of α. The entire region receives precipitation of more than 5 mm day^{-1} when α is less than 0.30. The precipitation north of 20° N is less than 5 mm day^{-1} for $\alpha = 0.40$ and 0.50 throughout the season.

Over the Indian landmass, monsoon begins across the southern peninsula in early June causing heavy precipitation. The northward propagation of the monsoon is due to a large scale transition of deep convection from equatorial to continental regions. The northwest extent of precipitation over India during JJAS is an important factor determining the overall agricultural production of the country. The mean JJAS precipitation decreases along the northwest direction and it would be worthwhile to compare the simulated northwest precipitation with observation for different relaxation parameters along the line (see Fig. 7). For comparisons, a bi-linear interpolation was performed to increase the number of points along the northwest. The magnitude of precipitation along the northwest direction over Indian landmass show a remarkable trend as α varies (Fig. 7). For values of $\alpha = 0.40$ and 0.50, the precipitation decreases much more rapidly along the direction than for the lower values. The slope of the simulated curve is the nearest to observation when $\alpha = 0.10$.

Figure 8 shows RMSE calculated over Indian and southeast Asian land and ocean as a function of α. The RMSE is least for $\alpha = 0.10$ and increases as α increases, over land and ocean. This is because the overestimation of precipitation over the region increases as α increases. Hence, it can be said that in terms of RMSE, the model

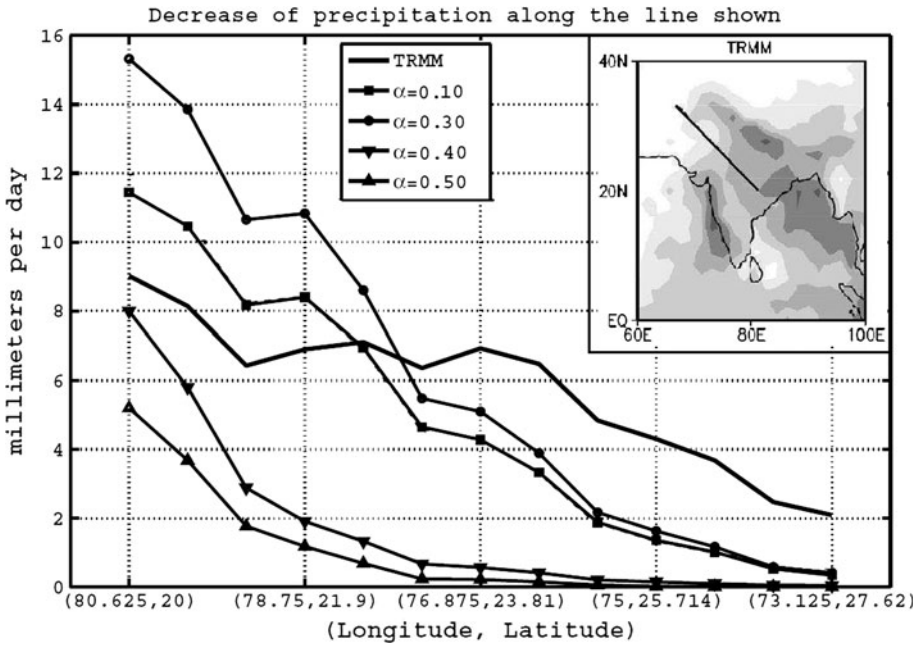

Fig. 7 Northwest extent of precipitation over Indian land along the line shown in the inset figure. Bi-linear interpolation was performed to obtain precipitation values along this line from regular angle grid. Precipitation for $\alpha = 0.20$ was not shown here for clarity (the curve for $\alpha = 0.20$ lies between that for 0.10 and 0.30)

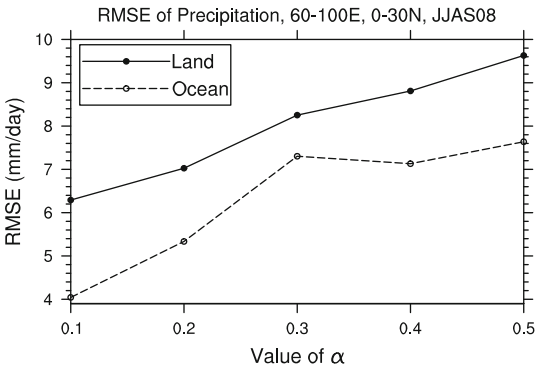

Fig. 8 RMS error in precipitation as a function of relaxation parameter (α) over India and southeast Asia

performs the best over these regions when α is set to 0.10. Its noteworthy to see that the RMSE is more over land when compared to ocean.

To get the precipitation ranges in which a particular value of relaxation parameter performs better over India and southeast Asia, two statistical scores, bias score and Equitable Threat Score (ETS) of precipitation, are plotted in Fig. 9. These scores are plotted in terms of monthly mean of June, July, August, and September of precipitation events to evaluate the subseasonal skill in the model simulation. The bias score is defined as

$$\text{BIAS} = \frac{F}{O} \tag{11}$$

where, F and O are the number of grid points over which forecast and observed precipitation exceed a specified threshold respectively. Bias signifies how well the frequency of simulated events compare to the observed frequency of those events. Bias varies from 0 to ∞, 1 representing a perfect score. ETS is defined as

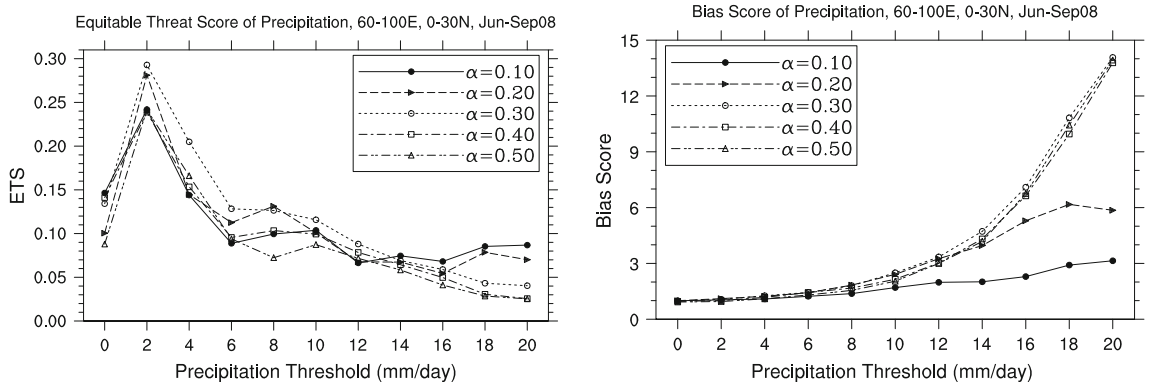

Fig. 9 Equitable threat score and bias score for different relaxation parameters (α) over India and southeast Asia

$$\mathrm{ETS} = \frac{H - E}{F + O - H - E}, \tag{12}$$

H is the number of grids points that correctly forecast more than the specified threshold (also termed as a hit); $E = F^{*}OT$, T being the total number of grids points over the region. While in general a higher ETS signifies a better skill, it is not always true. Mesinger (2008) and Brill (2009) have shown that it is possible to obtain a higher ETS by artificially increasing the error.

It can be seen in Fig. 9 that for very low-precipitation events (less than 2 mm day^{-1}), the simulated precipitation is not sensitive to α. In terms of ETS, the control experiment value of $\alpha(0.30)$ performs better for mid-range precipitation events (2–14 mm day^{-1}), while bias remains almost the same. In higher precipitation ranges (more than 14 mm day^{-1}), $\alpha = 0.10$ outperforms every other value by a significant margin. Hence, while lower values of α (less than 0.30) do not have significant effect over other regions of the tropics where the precipitation events mostly falls in the middle range, it performs better over highly precipitating regions like India and southeast Asia.

The zonal mean precipitation averaged over 60° E–100° E during JJAS, 2008 is shown in Fig. 10. It can be easily seen that, the simulation with $\alpha = 0.10$ comes closest to observation. The model is able to produce the observed local maxima and minima for $\alpha = 0.10$ and is the closest to observation. The RMSE between the simulated precipitation pattern and observation is least (1.6 mm day^{-1}) for $\alpha = 0.10$. The values of α greater than 0.20 produces a overestimation of precipitation at 10°N.

Based on the analysis till now, we can say that $\alpha = 0.10$ performs best over India and southeast Asia. However, to find out how the model performs with different values of α over different parts of tropics we choose six different regions indicated in Fig. 2. Figure 11 gives the magnitude of mean JJAS precipitation over these regions due to different values of α. The mean precipitation over tropics is largely unaffected by the choice of α. Over predominantly continental regions, viz India and central Africa, a lower α gives higher precipitation and it decreases with increasing α. Over oceanic regions, viz BoB and WP, the trend reverses and a increase in α increases precipitation. In terms of spatial mean precipitation, the simulation with $\alpha = 0.10$ comes closest to observation over the Indian landmass and BoB. $\alpha = 0.30$ gives the closest values for WP and American tropics, while $\alpha = 0.50$ comes closest for African tropics and EIO.

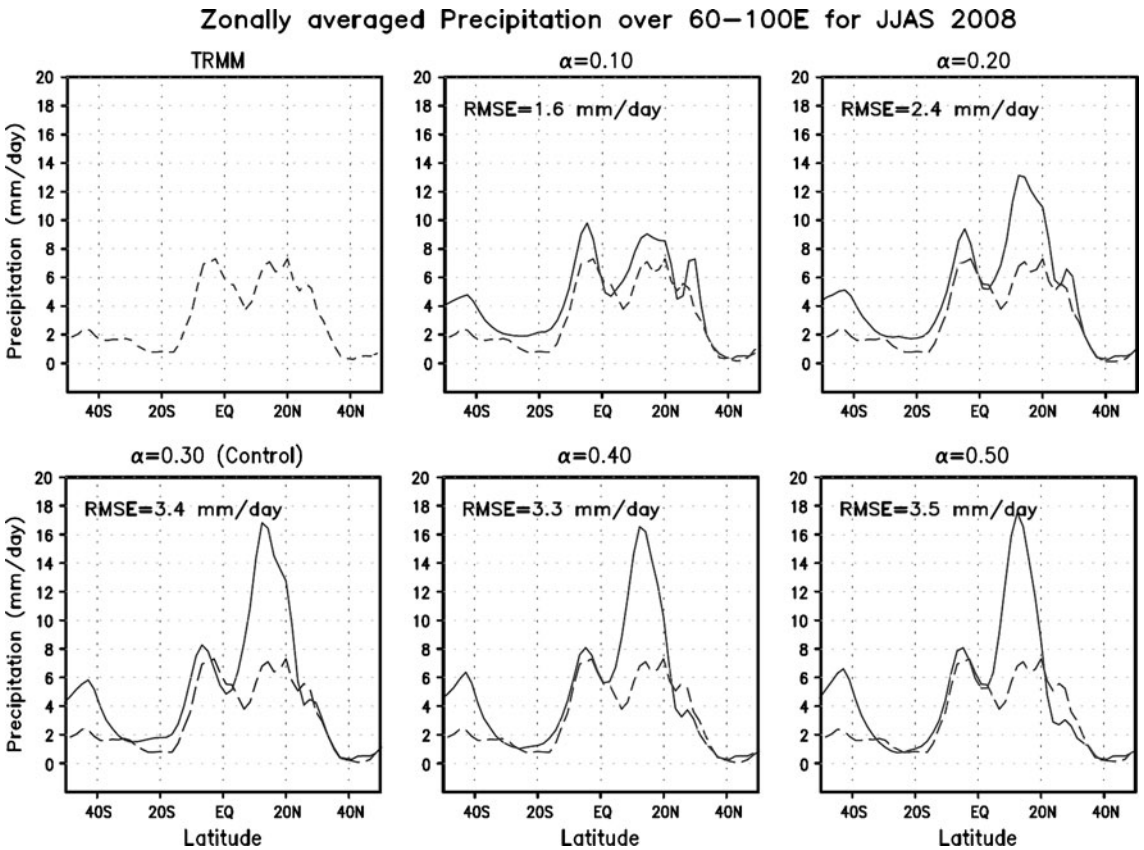

Fig. 10 Model simulated (*solid line*) zonal mean precipitation along 60°–100°E during JJAS 2008 (mm day^{-1}) as a function of latitude with different relaxation parameters compared to TRMM (*dashed line*)

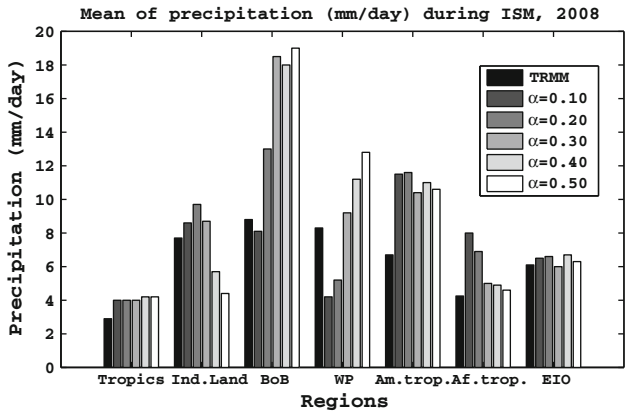

Fig. 11 Spatial mean of precipitation over different parts of the tropics from TRMM estimates and model simulations with different cloud relaxation parameters

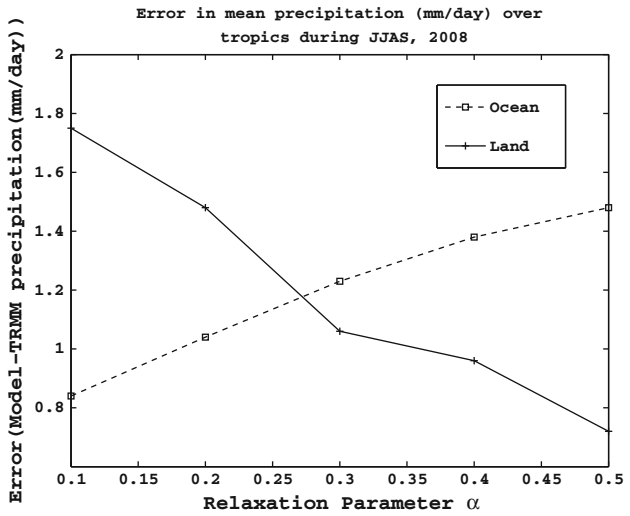

Fig. 12 Error in simulating spatial mean precipitation on land and ocean over the tropics as a function of relaxation parameter

In Fig. 11, we saw that the trend of precipitation with α was opposite over land and ocean. To ensure that this is true over the entire tropics, precipitation error is plotted separately over land and ocean as a function of α in Fig. 12. It can be seen that the error over land decreases and that over ocean increases monotonically as α increases. Hence, the simulated value of mean precipitation over land is closest to observation when α is largest while the opposite is true over oceans. Oceans act as a source of moisture and generally result in deeper clouds with higher convective activity (CAPE) when compared to land and this difference in intensity of convective activity over oceans and land is what we believe is the reason for this behavior. Going back to the definition of relaxation parameter (Eq. 1), we find that a cloud which takes longer time to adjust to the convective instability, should be represented by a lower value of relaxation parameter. If we assume that a deeper cloud takes longer time to adjust the environment, then a lower value of relaxation parameter would represent that cloud better in the model. Clouds over ocean are comparatively deeper than the clouds over land and hence we see the trend of precipitation in Fig. 12. This calls for a modification in the RAS scheme that takes into account the life time of the cloud in selecting relaxation parameter.

6.3 Cloud-type-dependent relaxation parameter

OLR is low in high-precipitation regions over the tropics and it represents regions of high convective activity. For the present study, we take the average of OLR for JJAS, 2008 over different parts of the tropics. On the days when there were no clouds and no precipitation, the clear sky OLR (which is very high compared to cloud top OLR over the tropics) was not considered while averaging. This method of averaging provides the seasonal mean OLR only during precipitation. Based on precipitation, six most convectively active regions over the tropics, viz Indian land, BoB, EIO, WP, American tropics, and African tropics were chosen for the study. The presence of precipitation on a particular day implies presence of clouds. We took a particular region and averaged the observed daily OLR over that region when model precipitation was greater than 0.10 mm day^{-1} for a particular day. We then compared the performance of the model simulated precipitation due to different relaxation parameters over these regions with observation (TRMM), taking RMSE as the basis.

Figure 13 shows the mean OLR over different regions with the corresponding values of α that gave least RMSE over that region. It can be seen that as the OLR increases, larger relaxation parameter is favored to represent the cloud adjustment time. In the model, multiple clouds are called and the effect of these clouds is averaged at each time step. Only the dominant cloud has maximum effect in the chosen region. This can be easily seen over the BoB (Fig. 13) where the deep convection is dominant during JJAS. Although shallow clouds are also present, the dominant clouds are the deep clouds. In effect, a lower relaxation parameter performs better. In RAS, a cloud type is distinguished by the level at which it detrains and not the fractional entrainment rate (or entrainment parameter λ defined in Arakawa and Schubert 1974). The deeper clouds have lesser entrainment (λ) than the shallower clouds and hence, lesser dilution from environmental air. Thus, the lifetime (or the adjustment time) of a deeper cloud is more than that of a shallower cloud. Following this argument and the result of Fig. 13, we assume a linear relation between cloud depth and relaxation parameter.

In the experiment, the cloud base was assumed to be at the second lowest layer in the model for all cloud types. A

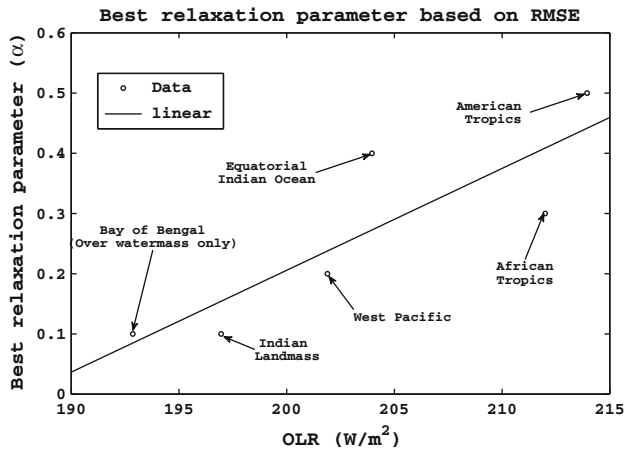

Fig. 13 The best relaxation parameter (α) based on RMS error in precipitation during June–September 2008 over different regions as a function of mean OLR over the same region. The OLR was averaged only when precipitation was present in a grid, which ensures presence of clouds

particular cloud can detrain at any level above its base. From Fig. 13, we find that over the six regions, the α with least RMSE varies between 0.10 and 0.60. Hence, here we assume a linear relation with boundary condition of $\alpha = 0.10$ for the deepest cloud and $\alpha = 0.60$ for the shallowest one, given by

$$\alpha(h) = a + b * h \tag{13}$$

where, h is the height index (in reverse order in the model, i.e., in a K-layer model, $h = K$ for the surface and it is 1 for the topmost layer). The relaxation parameter, $\alpha(h)$, is cloud-type-dependent. For a 28-layer model, when we fix $\alpha(26)$ as 0.60 and $\alpha(1)$ as 0.10, **a** and b takes the value of 0.08 and 0.02, respectively. In the model, whenever a cloud type is selected randomly for iteration, a corresponding α is selected for relaxing the environment.

Figure 14 shows model precipitation over the tropics after implementing the linear relaxation parameter. The RMSE due to a linear α is lowest when compared to the corresponding values of the fixed α cases that we tested shown in Fig. 4. The SC decreased from 0.70 in control experiment ($\alpha = 0.30$) to 0.64 which is an intermediate value between the lowest (0.61) and highest (0.70) values corresponding to $\alpha = 0.10$ and 0.30, respectively. The mean simulated precipitation over tropics is 4.21 mm day^{-1} over land, 3.97 mm day^{-1} over oceans, and 4 mm day^{-1} over land and oceans combined. These values are still large compared to corresponding TRMM values of 2.76, 2.96 and 2.91 mm day^{-1}. The model values are between simulated precipitation using the lowest ($\alpha = 0.10$) and highest ($\alpha = 0.50$) fixed values of relaxation parameter. The major impact of using a linear relaxation parameter is seen over Indian, southeast Asian and WP regions (Fig. 14).

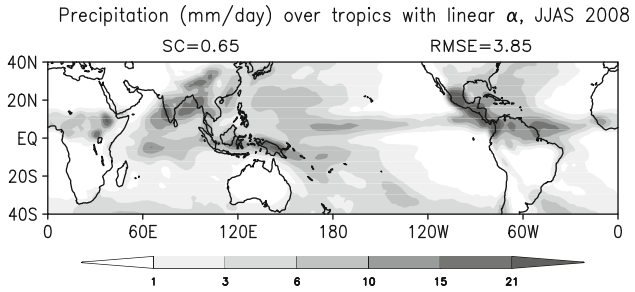

Fig. 14 Precipitation during June–September 2008 from model simulation with cloud-type-dependent relaxation parameter. The spatial correlation (SC) and RMS error (RMSE) of simulated precipitation, indicated at *top* of the panel, are calculated with respect to TRMM over the region 30°S–30°N, 0–360°E

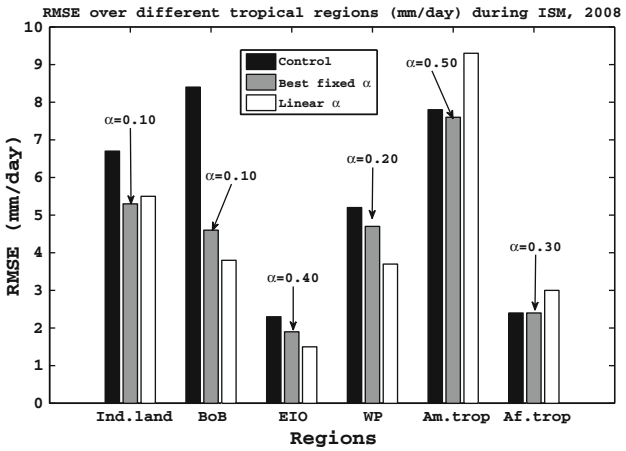

Fig. 15 Precipitation simulation comparison between control simulations, the best fixed relaxation parameter and the cloud-type-dependent relaxation parameter over the six chosen regions

Figure 15 shows the RMSE results over the 6 selected regions after implementing linear relaxation parameter. In 4 out of the 6 regions, viz BoB, Indian land, EIO and WP, the simulations are better than the control experiment ($\alpha = 0.30$). We see that using linear α, the simulations over BoB, EIO, and WP are better than the simulations with the best fixed α (with least RMSE) over the corresponding regions. However, over American and African tropics, the simulations give higher RMSE compared to control experiment. Hence, in terms of RMSE, a linear α improved the precipitation simulations over most parts of the tropics and hence improved performance over tropics as a whole.

The zonal mean of precipitation over India and southeast Asia during JJAS, 2008 is given in Fig. 16. The distribution is very close to observation (TRMM). The RMSE between the observed and simulated pattern is 1.8 mm day^{-1} which is slightly more than when α was set to 0.10 (Fig. 10) and substantially less than RMSE due to any other value of α. Furthermore, the simulated and observed distribution almost coincide over the region from 10°S to

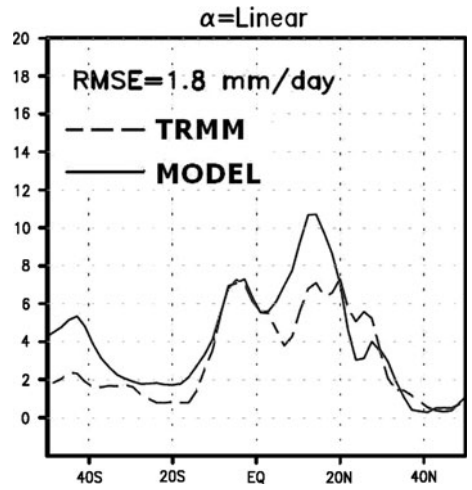

Fig. 16 Zonally averaged precipitation along 60°–100°E during JJAS 2008

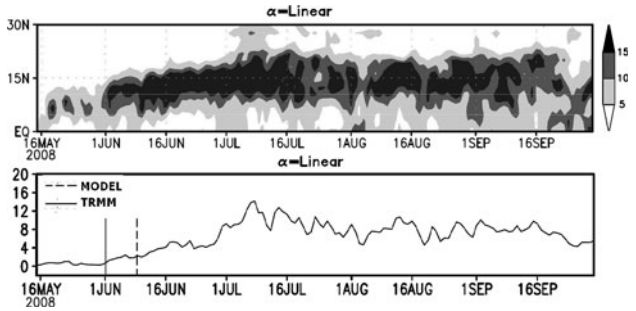

Fig. 17 Top: Zonally averaged precipitation (80°E–90°E) as a function of time with linear α; Bottom: time series of precipitation over Indian land (8°–28°N, 70°–90°E)

5°N for linear α. The onset of monsoon over Indian landmass due to linear α, (precipitation more than 3.5 mm day^{-1} persisting at least 1 pentad) as seen in Fig. 17, occurs on 7 June which is 7 days after the actual onset and 8 days after that of the control experiment. In Indian summer monsoon season, the rainfall peaks in the months of July and August. This pattern is simulated better by the model when using a linear α than for values of $\alpha = 0.30$ and above (see Fig. 5).

6.4 Precipitation-SST relationship

Gadgil et al. (1984) identified sea surface temperature (SST) as the most important factor controlling the generation and maintenance of large-scale and synoptic-scale cloudiness in the tropics. We have plotted precipitation as a function of SST over the tropics in Fig. 18 for different values of α. Below 25.25°C, all the curves nearly coincide and the precipitation remains insensitive to α. After 26.75°C, however, the precipitation increases strongly with

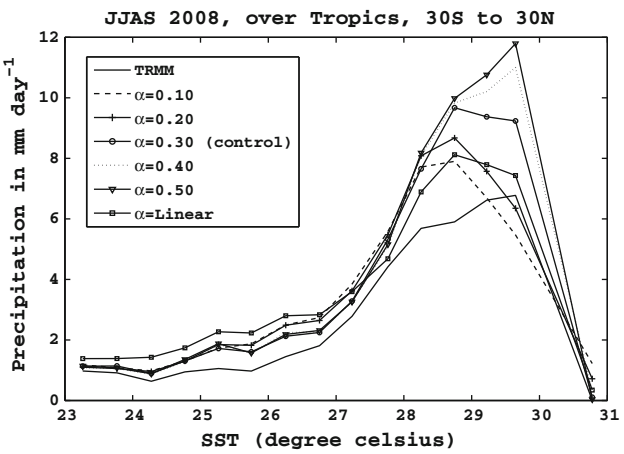

Fig. 18 Precipitation-SST relationship over the Tropics (30°S–30°N) from observational estimates and model simulations with different relaxation parameters during JJAS 2008

SST and peaks in the range of 28–30°C. The observed peak occurs at 29.75°C with the peak value of 6.8 mm day^{-1}. The peak values for $\alpha = 0.10$, 0.20 and 0.30 are 7.9, 8.63, 9.67 mm day^{-1} at 28.75°C and 11 and 11.8 mm day^{-1} for $\alpha = 0.40$ and 0.50 at 29.75°C, respectively. Hence, $\alpha = 0.10$ comes closest in simulating peak precipitation for a given SST, though the peak occurs earlier at 28.75°C. The precipitation as a function of SST due to linear α in Fig. 18 over tropics show that the simulated functional dependence over the region is better than the curves by any fixed α values above 27°C and comes closest to the observation. Whereas, with $\alpha = 0.10$, the precipitation starts decreasing rapidly after 28.75° C, the decrease is not as steep as that for linear α and the slope above 29.75°C is almost same as that in observation.

7 Conclusions

In the present study, we tested the sensitivity of precipitation simulation by SFM on the choice of relaxation parameter value. We found that simulations are highly sensitive over most parts of the tropics. We started by looking at the effect of different spatially fixed values for relaxation parameter on the precipitation simulations. It was found that in the control simulation with $\alpha = 0.30$, the model was over-estimating the precipitation over most parts of the tropics, especially over Indian landmass, BoB, southeast Asia, WP, and American tropics. We varied α from 0.10 to 0.50 in steps of 0.10 and simulated the precipitation for JJAS, 2008. It was seen that over tropics, the RMSE decreased as α was decreased from 0.50 to 0.20 and then increased for 0.10. The best SC of 0.70 was obtained with $\alpha = 0.30$. The SC also decreased when α was decreased. Of all the fixed values of α, 0.10 produced least

RMSE over India and southeast Asia. It also produced the spatial coverage of precipitation over India most realistically. The skill matrices like ETS and bias score over India and southeast Asia showed that for the simulation of precipitation events in the range 2–14 mm day^{-1}, $\alpha = 0.30$ performed better than the other values of α, while for the higher precipitation ranges of more than 14 mm day^{-1}, $\alpha = 0.10$ performed best.

Simulated precipitation with $\alpha = 0.10$ came closest to TRMM over India and southeast Asia compared to any other fixed value of α for the zonally averaged precipitation. The relaxation parameter value, $\alpha = 0.10$, also simulated the maxima and minima of precipitation over this region closest to the observation. In terms of RMSE, $\alpha = 0.10$ gives the best result (least RMSE). Due to improvement in precipitation, the variables in the model which are derived from precipitation, such as cloud fraction (Slingo 1987) also showed improvement. As the focus of the present study was the effect of α on precipitation alone, the discussion of results for other variables derived from precipitation will be presented in a separate study.

The choice of α had a very significant effect on the precipitation–SST relationship over the tropics. The precipitation–SST relationship for $\alpha = 0.10$ came closest to the observed relation and the maximum of rainfall was also closest to observations. The peak precipitation increased when α was increased. It was also seen that the mean tropical precipitation over land decreased and that over ocean increased when α was increased from 0.10 to 0.50. We believe the difference in intensity of convective activity to be the reason for this behavior. To understand this behaviour, we examined the definition of relaxation parameter closely. We selected six convectively active regions over the tropics, viz African tropics, West Pacific, Indian land, Bay of Bengal, equatorial Indian ocean and American tropics. Based on the RMSE, it was found that there is no one universal value of α which performed better than the other over different parts of the tropics and different values performed well over different parts of the tropics. We also found that the regions where the OLR was low (representing deeper clouds), a lower value of relaxation parameter gave better results in terms of RMSE. As OLR can be used as a proxy for cloud depth, we proposed a linear relation between α and the cloud depth. Implementing this cloud type dependent α in the model improved the model performance over the tropics in terms of mean RMSE. Four out of the selected six regions showed lower RMSE than the least obtained from any fixed value of α. The major improvement was seen over Indian and Asian region where the model showed precipitation closest to TRMM.

The new cloud-type-dependent linear relaxation parameter also produced one of the best distribution of zonally averaged precipitation over India and southeast Asia second only to $\alpha = 0.10$. The precipitation–SST relationship over the tropics was one of the best with linear relaxation parameter. Furthermore, a cloud-type-dependent relaxation parameter is physically more realistic than a fixed value for all cloud types and should be preferred over a fixed value for all cloud types in the model.

The partitioning of total precipitation between convective and stratiform components was found insensitive to the choice of relaxation parameter. Convective precipitation component contributed more than 80% of the total precipitation irrespective of the value of the relaxation parameter. In the present study, we empirically assumed a linear cloud type dependent relaxation parameter. At this point, we emphasize a need for a better functional dependence based on observations and experiments which can improve short time to seasonal prediction during Indian summer monsoon.

Acknowledgements DKJ and RSN thank INCOIS and MoES, and AC thanks ISRO MTUP for supporting this research.

References

Adler RF, Huffman G (2000) Tropical Rainfall Distributions Determined Using TRMM Combined with Other Satellite and Rain Gauge Information. J Appl Meteorol 39:2007–2023

Alpert J, Kanamitsu M, Caplan P, Sela J, White G (1988) Mountain induced gravity wave drag parameterization in the NMC medium-range forecast model. Conference on numerical weather prediction, 8th, Baltimore, MD, pp 726–733

Anthes RA (1977) A cumulus parameterization scheme utilizing a one-dimensional cloud model. Mon Wea Rev 105:270–286

Arakawa A, Schubert W (1974) Interaction of a cumulus cloud ensemble with the large-scale environment, Part I. J Atmos Sci 31(3):674–701

Bhanu Kumar O, Ramalingeswara Rao S, Ranganathan S, Raju S (2010) Role of intra-seasonal oscillations on monsoon floods and droughts over india. Asia Pac J Atmos Sci 46:21–28

Brankovic Č, Palmer T (1997) Atmospheric seasonal predictability and estimates of ensemble size. Monthly Weather Rev 125(5):859–874

Brill K (2009) A general analytic method for assessing sensitivity to bias of performance measures for dichotomous forecasts. Weather Forecast 24(1):307–318

Chakraborty A, Nanjundiah RS, Srinivasan J (2002) Role of Asian and African orography in Indian summer monsoon. Geophys Res Lett 29(20):50–51

Chou M (1992) A solar radiation model for use in climate studies. J Atmos Sci 49:762–772

Chou M, Suarez M (1994) An efficient thermal infrared radiation parameterization for use in general circulation models. NASA Tech Memo 104606(3):85

Das S, Mitra A, Iyengar G, Mohandas S (2001) Comprehensive test of different cumulus parameterization schemes for the simulation of the Indian summer monsoon. Meteorol Atmos Phys 78(3):227–244

Gadgil S, Joshi N, Joseph P (1984) Ocean-atmosphere coupling over monsoon regions. Nature 312:141–143

Grell G (1993) Prognostic evaluation of assumptions used by cumulus parameterizations. Monthly Weather Rev 121(3):764–787

Hong S, Pan H (1996) Nonlocal boundary layer vertical diffusion in a medium-range forecast model. Monthly Weather Rev 124(10): 2322–2339

Huffman G, Adler R (2007) The TRMM multisatellite precipitation analysis (TMPA): quasi-global, multiyear, combined-sensor precipitation estimates at fine scales. J Hydrometereol 8:38–55

Kanamitsu M, et al. (2002) NCEP dynamical seasonal forecast system 2000. Bull Am Meteorol Soc 83(7):1019–1037

Kang I, et al. (2002) Intercomparison of the climatological variations of Asian summer monsoon precipitation simulated by 10 GCMs. Clim Dyn 19(5):383–395

Krishnamurti TN, Ramanathan Y, Pan HL, Pasch RJ, Molinary J (1980) Cumulus parameterization and rainfall rates I. Monsoon Weather Rev 108:465–472

Kummerow C, Barnes W, Kozu T, Shiue J, Simpson J (1998) The tropical rainfall measuring mission (TRMM) sensor package. J Atmos Ocean Technol 15(3):809–817

Lee J, Pierrehumbert R, Swann A, Lintner B (2009) Sensitivity of stable water isotopic values to convective parameterization schemes. Geophys Res Lett 36

Lord S, Arakawa A (1980) Interaction of a cumulus cloud ensemble with the large-scale environment. Part II. J Atmos Sci 37: 2677–2692

Martin G, Soman M (2000) Effects of changing physical parameterization schemes on the simulation of the Asian summer monsoon in the UK Met Office unified model. Hadley Centre Tech. Note HCTN17

Mesinger F (2008) Bias adjusted precipitation threat scores. Adv Geosci 16:137–142

Mishra S, Srinivasan J (2010) Sensitivity of the simulated precipitation to changes in convective relaxation time scale. Ann Geophys 28:1827–1846

Moorthi S, Suarez M (1992) Relaxed Arakawa-Schubert- A parameterization of moist convection for general circulation models. Monthly Weather Rev 120(6):978–1002

Pan H, Mahrt L (1987) Interaction between soil hydrology and boundary-layer development. Boundary Layer Meteorol 38(1): 185–202

Pan H, Wu W (1995) Implementing a mass flux convection parameterization package for the NMC medium-range forecast model. NMC Office Note 409(40):20,233–9910

Pattanaik VS (2004) Sensitivity of Indian monsoon rainfall to different convective parameters in the Relaxed Arakawa Schubert scheme. IITM research report no. RR-105

Rajendran K, Nanjundiah R, Srinivasan J (2002) Comparison of seasonal and intraseasonal variation of tropical climate in NCAR CCM2 GCM with two different cumulus schemes. Meteorol Atmos Phys 79(1):57–86

Ratnam J, Kumar K (2005) Sensitivity of the simulated monsoons of 1987 and 1988 to convective parameterization schemes in MM5. J Clim 18:2724–2743

Ratnam J, Sikka D, Banerjee S (2009) Simulation of 2006 monsoon using T170L42 AGCM: sensitivity to convective parameterization schemes. Int J Climatol 29(2):289–303

Reynolds RW, Smith TM (1994) Improved global sea surface temperature analyses using optimum interpolation. J Climate 7:929–948

Slingo J (1987) The development and verification of a cloud prediction scheme for the ECMWF model. Q J R Meteorol Soc 113(477):899–927

Sperber K, Palmer T (1996) Interannual tropical rainfall variability in general circulation model simulations associated with the Atmospheric Model Intercomparison Project. J Clim 9(11): 2727–2750

Tebaldi C, Knutti R (2007) The use of the multi-model ensemble in probabilistic climate projections. Phil Trans R Soc A Math Phys Eng Sci 365(1857):2053

Tiedtke M, Heckley WA, Slingo J (1988) Tropical forecasting at ECMWF-The influence of physical parameterization on the mean structure of forecasts and analyses. Q J R Meteorol Soc 114:639–664

Zhang G, McFarlane N (1995) Sensitivity of climate simulations to the parameterization of cumulus convection in the Canadian Climate Centre general circulation model. Atmos Ocean 33:407–407